Spatial and Temporal Analyses of Citrus Tristeza Virus in Eastern Spain

T. R. Gottwald, M. Cambra, P. Moreno, E. Camarasa, and J. Piquer

First author: research plant pathologist, USDA, Agricultural Research Service, Orlando, FL 32803; and second, third, fourth, and fifth authors: research plant pathologists, Instituto Valenciano de Investigaciones Agrarias (IVIA), Apartado Oficial, 46113 Moncada (Valencia), Spain.

This work was funded by CAICYT (project 727); Spain-USA Committee for Scientific and Technical Cooperation (grant 156); Commission of the European Communities, contract N. CT90-0783 and INVA (projects 8179 and SC94-035). T. R. Gottwald visited IVIA to analyze the data presented here and was supported by a fellowship from the Consellería de Cultura, Educación y Ciencia de la Generalitat Valenciana.

We thank T. Gorris and M. E. Martinez of IVIA, Moncada, Valencia, and P. Bell, USDA, ARS, Orlando, FL, for technical assistance in collecting and processing samples and data and G. Hughes, D. Chellemi, and S. Nelson for help with interpretation of results of beta-binomial, geostatistical, and two-dimensional distance class analyses, respectively.

Accepted for publication 25 September 1995.

ABSTRACT

Gottwald, T. R., Cambra, M., Moreno, P., Camarasa, E., and Piquer, J. 1996. Spatial and temporal analyses of citrus tristeza virus in eastern Spain. Phytopathology 86:45-55.

Citrus tristeza virus (CTV) was monitored for up to 14 years by monoclonal antibody probes via enzyme-linked immunosorbent assay in five orange and grapefruit orchards with symptomless trees in Valencia and Alicante provinces, Spain. Linear, exponential, logistic, or Gompertz nonlinear temporal models were selected as the most appropriate, depending on the phase of the epidemic during the assessment period and based on correlation of observed versus predicted values and examination of the patterns of residual error. Ordinary runs analysis for within- or across-row association of CTV-positive trees indicated that the disease status of immediately adjacent trees was unpredictable. The beta-binomial index of dispersion for different quadrat sizes indicated a tendency for aggregations of infected trees at quadrat sizes of 2 × 2 or 4 × 4 CTV-positive trees in some plots, which when viewed with ordinary runs suggested the possible presence of longer distance spatial relationships. Two-dimensional distance class (2DCLASS) analysis indicated a random spatial pattern of CTV incidence and general lack of association of infection among adjacent trees. Spatio-temporal distance class (STCLASS) analysis further indicated a lack of spatial dependency among adjacent CTV-positive trees over time. Significant edge effects detected by both 2DCLASS and STCLASS analyses suggested possible spread of CTV from inoculum originating outside the area of the individual plots. Semivariograms from spatio-temporal geostatistical analyses of four directions of orientation confirmed a lack of spatial dependency of infection among adjacent or nearby trees over time. These combined spatial and temporal analyses gave some insight into possible underlying processes of CTV spread and suggested CTV spread must be predominantly to trees farther away rather than to immediately adjacent trees. If a nonrandom spatial structure of CTV incidence does exist, it may well be of a complexity beyond the detection ability of the spatial analysis methods employed or perhaps on a scale that is larger than the dimensions of the plots studied.

Additional keywords: anisotropy, *Aphis gossypii*, beta-binomial distribution, geostatistics.

By 1987, throughout the world, over 50 million citrus trees grafted on sour orange were killed due to severe decline-inducing isolates of citrus tristeza virus (CTV), confirming CTV as one of the most destructive diseases of citrus. In Spain, CTV was first recognized as a problem in 1957 after a severe freeze in 1956 in the Ribera Alta District, Valencia; it was especially severe on sweet orange and mandarins grown on sour orange rootstock (9,39,40). Since that time, CTV has spread throughout much of Spain by movement of infected budwood and vectors and has caused the death of more than 17 million trees (5). Citrus nurseries in Spain have been forbidden to propagate sweet orange, mandarin, and grapefruit on sour orange since 1968. A program to obtain and propagate virus-free varieties has subsequently been established (42). This policy has resulted in the systematic replacement of trees that have died or are in severe decline with replants on Carrizo, Troyer citrange, or other tolerant rootstocks (20).

The continued spread of CTV is of concern to Valencian growers since about 40% of the 170,000 ha of citrus (approximately 80 million trees) grown in the region are sweet orange or mandarin on sour orange rootstock (58). The natural movement of CTV is related to the presence of *Aphis gossypii* Glover, *A. spiraecola* Patch, *Toxoptera aurantii* (Fons.), and *T. citricida* (3,28, 31,46,55,57). The most efficient vector of CTV worldwide is *T. citricida* (46,56). However, *A. gossypii* is the most efficient vector of CTV in Spain, California, Florida, Israel, and in all other locations where *T. citricida* is absent and in which *A. gossypii* transmission has been studied (2,3,28,29,31,46,55). Vector efficiency and transmission studies combined with aphid-trapping studies in citrus have demonstrated that *A. gossypii* populations in citrus are more than sufficient to account for the CTV increase observed (17,18). Recent increases in *A. gossypii* populations in Spain coincided with the spread of CTV (31; M. Cambra and E. Camarasa, *unpublished data*). *A. gossypii* spreads CTV isolates from Spain more efficiently than other aphid species (28), and *A. gossypii* is responsible for transmission of severe CTV strains in Spain, California, Florida, and Israel (1,2,46,55,57). Although cit-

Corresponding author: T. R. Gottwald
E-mail address: tgottwald@asrr.arsusda.gov or gott@magicnet.net

Publication no. P-1996-1130-01R

rus is a host for *A. gossypii*, it is not the preferential host (57). Unlike other aphid species common to citrus, *A. gossypii* does not heavily colonize citrus (30,48,57). *A. gossypii* rarely forms apterous colonies on citrus and most often migrates through orchards from surrounding areas or crops such as cotton, cucurbits, and vegetables (48,57). Only a few nonwinged *A. gossypii* are usually found in citrus groves, and therefore, a person is more likely to encounter alate *A. gossypii* that are foraging in the orchard than to find apterous colonies inhabiting citrus flush (57). Peak trapping periods for *A. gossypii* in citrus plantations usually correspond to two or more seasonal periods of alate migration (30, 31,48).

Due to the long perennial duration of most tree-crop epidemics, only a few have been modeled over time. Temporal and spatial analyses have been conducted for a few citrus diseases, such as citrus canker and greening (22,25,26,27). For CTV, modeling and simulations have been attempted previously but only from limited data (12,14,37,40). A preliminary analysis of a portion of the data presented in this report with less rigorous analytical techniques and for fewer years has been published previously (24).

The study of viral and other graft-transmissible, fastidious pathogens of tree crops often dictates the use of serological or molecular probes for pathogen detection and confirmation. The development of monoclonal antibodies (MAbs) and the use of enzyme-linked immunosorbent assay (ELISA) for diagnosis of CTV have provided new opportunities for epidemiology research, because the rapid detection and confirmation of large numbers of samples have become feasible (6,7,8,10,14,19,21,24,40,52,53). Data resulting from these analyses represent the presence or absence of the pathogen and, thus, are binary (+/–). Several statistical procedures exist for the quantitative analysis of spatial patterns of disease at a single point in time. Ordinary runs analysis, which utilizes binary data, is the preferred method for unidirectional analysis to assess the presence or absence of aggregation of diseased individuals within columns and within rows in a population of diseased plants (36). Recently the beta-binomial discrete distribution has been demonstrated to be more appropriate than the negative binomial distribution to examine spatial patterns of disease incidence, i.e., binary data, for the presence of aggregation

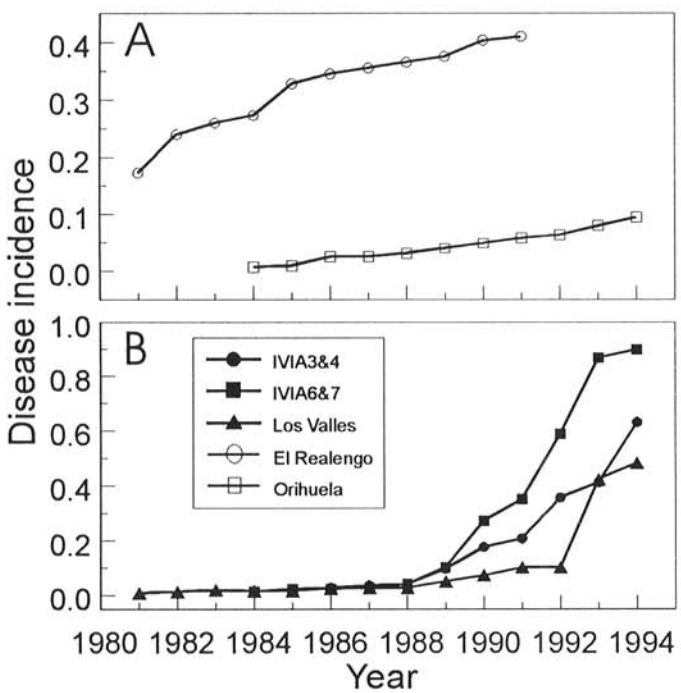

Fig. 1. Temporal disease progress of citrus tristeza virus in five citrus orchards in eastern Spain. Disease incidence for all trees in each orchard was assessed by double-antibody sandwich-enzyme-linked immunosorbent assay.

(32,35).

Two-dimensional distance class analysis (2DCLASS) is based on binary data collected from a rectangular matrix to characterize the spatial relationships among diseased plants and, therefore, is well suited for analyzing data from fastidious diseases of tree crops (11,12,41,44,45). Spatio-temporal distance class analysis (STCLASS), an outgrowth of 2DCLASS, has been developed recently to compare the spatial pattern of diseased plants between two assessment dates (43).

Geostatistics is a type of spatial analysis based on regionalized variables, i.e., variables depending on spatial position, and has been used in many fields of study, including geography, geology, and soil science. Geostatistics has been adapted recently to entomological and plant pathological applications (13,23,33,41,47,49, 50,54). Geostatistical results are often presented in semivariograms, which represent the average of squared differences in values between pairs of samples separated by a given distance (13, 15,16,23,38,47,49,50). The intent of such an analysis is to detect spatial dependence by measuring the variation of regionalized variables among samples separated by the same distance (41, 47,49). Semivariograms also can be calculated for specific directions to test for anisotropy, a characteristic of regionalized variables that do not have the same properties in all directions. Anisotropy associated with plant diseases can be interpreted as indicative of directional spread (38,47,49). By fitting the resulting semivariance data to theoretical transitional models used commonly in geostatistical analysis, interpretations can be made concerning the structure of the spatial data and inferences drawn concerning the spatial relationships among plants over a range of distances, i.e., spatial lags. However, the biological significance of these models is unclear, especially for data that lacks spatial associations among adjacent or nearby plants (41). Within plant pathology, geostatistics also has been used to examine the spatio-temporal characteristics of an epidemic for which diseased plants were assigned a value corresponding to length of time infected (50). The strength of this technique is the ability to examine the spatio-temporal relationships of diseased plants over the duration of an epidemic consisting of several assessment dates.

More detailed estimates of the rate of temporal increase of CTV in Mediterranean climates is needed to evaluate the expected productive life of a citrus orchard affected by tristeza. In addition, knowing the range of temporal rates of CTV is useful for existing disease-suppression/eradication programs. For such programs, rates of CTV-infected tree removal are based on the estimated temporal rates needed to offset disease increase and, thereby, suppress disease. Also, in disease-suppression programs, questions often are raised concerning the benefit of removing trees immediately adjacent to known CTV-infected trees to eliminate presymptomatic or nondetectable infections, i.e., those below the virus titer level necessary for serological detection. Clearly, a greater understanding of the spatial and spatio-temporal dependency of CTV is needed to address this issue.

The purpose of this study was to examine the spatial, temporal, and spatio-temporal dynamics of CTV in tolerant scion-rootstock combinations in the Valencia region of Spain in an attempt to determine likely rates of disease increase and spatial patterns of spread and, through detailed analysis, to better understand dissemination of CTV over time and space in the presence of aphid vectors, especially *A. gossypii*. For the purposes of investigation, we assumed the hypothesis that the spatial distribution of CTV incidence is aggregated through time, as is common for the majority of plant diseases.

MATERIALS AND METHODS

Data were collected over a 14-year period from five plantings: four in Valencia Province and one in Alicante Province, Spain. All plantings were on Troyer citrange or Cleopatra mandarin root-

stocks and, therefore, were symptomless for CTV. All of the plots were established from indexed CTV-negative mother plants and were disease-free when planted. All plots were assayed annually. Two of the test plots, IVIA3&4 and IVIA6&7, consisted of 216 trees each of Washington navel orange on Troyer citrange planted in 1978 on a 2 × 6-m spacing. Both plots were located on the grounds of the Instituto Valenciano de Investigaciones Agrarias, near Moncada, Valencia, Spain, and were assayed yearly from 1981 to 1994. The El Realengo plot consisted of 400 Marsh seedless grapefruit on Troyer citrange planted in 1973 on a 5.5 × 5.5-m spacing located on the El Realengo citrus farm in the Ribera Alta District in southern Valencia. In 1980, indexed CTV-free trees of Redblush grapefruit on Troyer citrange were interplanted among the rows. These trees were removed in 1991. The El Realengo plot was assayed yearly from 1981 to 1992. The Los Valles plot consisted of 408 Navelina orange on Cleopatra mandarin planted on a 6.5 × 4.0-m spacing located near Sagunto, Valencia, established in 1973 and was assayed yearly from 1981 to 1994. The Orihuela plot consisted of 346 trees of Newhall navel orange on Troyer citrange interplanted in 1979 among the rows of an older navel-on-sour orange planting located in Orihuela, Alicante. This former planting was established in a 6 × 4-m spacing, and the interplanted trees on Troyer citrange followed the same pattern. About 5% of the older trees were CTV-infected at replanting. Most of the CTV-infected trees had been topworked to lemon as soon as tristeza symptoms began to appear. This plot was bordered by lemon plantings on two sides, vegetable crops on one side, and a planting of sweet orange on sour orange on the fourth side and was assayed yearly from 1984 to 1993.

Traditional aphid-control procedures were used in all plots and consisted of spraying two to six times per year, depending on aphid population numbers, with dimethoate, methyl-oxidimethon,

TABLE 1. Nonlinear regression analyses of the incidence of citrus tristeza virus detected by enzyme-linked immunosorbent assay in five citrus orchards in eastern Spain

Model[a]	Plot	Parameter	Parameter estimate	Asymptotic standard error	Asymptotic 95% confidence interval		r^{*2}[b]	Residual pattern[c]
					Lower	Upper		
Lin	El Realengo	*r*	0.0218	0.0019	...	...	0.966	–
Lin	Los Valles	*r*	0.0267	0.0065	...	...	0.776	+
Lin	Orihuela	*r*	0.0081	0.0009	...	...	0.952	–
Lin	IVIA3&4	*r*	0.0541	0.0079	...	...	0.907	+
Lin	IVIA6&7	*r*	0.0938	0.0131	...	...	0.914	+
E	El Realengo	*r*	0.5771	0.0347	0.4998	0.6544	0.695	+
E	Los Valles	*r*	0.4378	0.0056	0.4255	0.4501	0.954	+
E	Orihuela	*r*	0.4201	0.4201	0.3949	0.4454	0.954	+
E	IVIA3&4	*r*	0.5968	0.0082	0.5787	0.6149	0.961	–
E	IVIA6&7	*r*	0.6414	0.0120	0.6150	0.6678	0.900	+
M	El Realengo	*r*	0.0623	0.0057	0.0496	0.0750	0.981	–
M	Los Valles	*r*	0.0171	0.0043	0.0076	0.0265	0.759	+
M	Orihuela	*r*	0.0068	0.0006	0.0056	0.0081	0.950	–
M	IVIA3&4	*r*	0.0407	0.0069	0.0256	0.0558	0.884	+
M	IVIA6&7	*r*	0.0738	0.0166	0.0372	0.1104	0.872	+
L	El Realengo	*r*	0.6726	0.0544	0.5513	0.7939	0.763	+
L	Los Valles	*r*	0.4745	0.0079	0.4572	0.4918	0.963	+
L	Orihuela	*r*	0.4293	0.0119	0.4025	0.4562	0.955	–
L	IVIA3&4	*r*	0.6792	0.0078	0.6620	0.6964	0.990	–
L	IVIA6&7	*r*	0.8159	0.0083	0.7976	0.8342	0.994	–
G	El Realengo	*k*	0.0600	0.0058	0.0470	0.0730	0.963	–
G		*B*	1.6339	0.0651	1.4868	1.7811		
G	Los Valles	*k*	0.2868	0.0377	0.2037	0.3698	0.973	–
G		*B*	45.1112	21.4016	–1.9936	92.2159		
G	Orihuela	*k*	0.0724	0.0067	0.0569	0.0879	0.977	–
G		*B*	5.3965	0.3244	4.6484	6.1447		
G	IVIA3&4	*k*	0.2991	0.0288	0.2349	0.3632	0.986	–
G		*B*	15.6480	4.0277	6.6737	24.6223		
G	IVIA6&7	*k*	0.5798	0.0632	0.4391	0.7206	0.990	–
G		*B*	88.0149	46.1469	–14.808	190.8373		
W	El Realengo	*a*	0.0000	...	...	...	...	
W		*b*	51.2569	5.4624	38.9000	63.6138	0.992	–
W		*c*	0.4167	0.0202	0.3710	0.4624		
W	Los Valles	*a*	0.0000	...	...	...	...	
W		*b*	15.4156	0.4563	14.4114	16.4199	0.966	–
W		*c*	5.4843	0.8450	3.6243	7.3442		
W	Orihuela	*a*	0.0000	...	...	...	...	
W		*b*	47.8115	10.0352	24.6700	70.9529	0.973	–
W		*c*	1.6481	0.2048	1.1758	2.1204		
W	IVIA3&4	*a*	0.0000	...	...	...	...	
W		*b*	11.3665	0.2016	10.9173	11.8158	0.992	–
W		*c*	3.8467	0.2977	3.1833	4.5101		
W	IVIA6&7	*a*	0.0000	...	...	...	...	
W		*b*	9.1298	0.0843	8.9420	9.3176	0.996	–
W		*c*	5.2432	0.3752	4.4073	6.0792		

[a] Model parameters were estimated by nonlinear regression of integrated equations: $y = y_0 rt$, $y = y_0 e^{rt}$, $y = 1 - (1 - y_0)e^{rt}$, $y = 1/(1 + \exp^{-[\ln(y_0/(1 - y_0)] + rt})$, $y = \exp^{-Be^{-kt}}$, and $y = 1 - \exp^{-[(t - a)/b]^c}$, for the linear (Lin), exponential (E), monomolecular (M), logistic (L), Gompertz (G), and Weibull (W) models, respectively, where *r* and *k* are rate parameters, *y* is disease measured as incidence of diseased trees, and *t* is time in years. For the Gompertz model, $B = -\ln(y_0)$. For the Weibull model, it was necessary to fix *a* at 1 to estimate *b* and *c* to allow the model to converge for some of the data sets.

[b] r^{*2} = coefficients of determination of correlation of predicted values against observed values to examine appropriateness of models.

[c] Presence (+) or absence (–) of patterns in the plots of the residuals of nonlinear regression over time.

imiadoprin, carbemma oxyprimide, or cipermethrin at recommended rates.

Sample collection and serological analysis. All trees in each plot were sampled yearly during May. Two to four young apical shoots, 10 cm long, were collected from different parts of each tree and were analyzed by the procedure described previously (10). Conventional double-antibody sandwich-ELISA (DAS-ELISA) methods with polyclonal antibodies from different antisera sources were used in 1981 and 1982. From 1983 to 1989, DAS-ELISA was performed with MAb 3DFI (52,53). From 1989 to the present, the analysis was done by the DAS-ELISA biotin/streptavidin system using a commercially available mixture of MAbs 3DFI and 3CA5 (Ingenasa Co., Madrid) (6,8).

Temporal analysis. Disease incidence (number of CTV-infected trees divided by total number of trees in the plot) of each plot was calculated for each year. The appropriateness of the linearized form of the linear, exponential, monomolecular, logistic, and Gompertz models was examined by linear regression analysis of transformed disease incidence data (4,11,34,51). Preliminary results from the linear regression analysis allowed the selection of parameters for the nonlinear regression analysis. Nonlinear regression analysis of nontransformed data from each plot was performed for the nonlinear forms (derivatives) of the same models (SAS NLIN procedure using the DUD option, SAS Institute, Cary, NC, version 6.04). In addition, the Weibull nonlinear model was fitted to the data sets. The appropriateness of each model was determined by examining the coefficient of regression, the correlation coefficient of observed versus detransformed predicted values, and the plots of residual errors versus predicted values. General model types were selected based on the shape of the disease progress curve. Models were further evaluated for the highest coefficient of correlation and were chosen as superior if no patterns were found in the residual plots (11,34).

Spatial analysis. Preliminary spatial analyses were used to examine whether aggregation of immediately adjacent diseased trees was present. More detailed analyses, aimed at examining more complex spatial relationships over longer distances, were used subsequently. Ordinary runs analyses were performed on each data set to determine whether aggregation existed between adjacent diseased trees within- or across-rows (36). A nonrandom pattern (i.e., aggregation) of diseased trees was assumed for a particular row if the observed was less than the expected number of runs at $P = 0.05$. To examine the data for the presence of aggregation at different spatial scales, the disease incidence data from each plot

TABLE 2. Ordinary runs analysis of citrus tristeza virus in four citrus orchards in eastern Spain[a]

Plot	Direction	No. of rows tested	Year of assessment[b]													
			1981	1982	1983	1984	1985	1986	1987	1988	1989	1990	1991	1992	1993	1994
IVIA3&4	N-S	12	...[c]	...	...	0	0	0	0	0	0	0.25	0.25	0.08	0.08	0
	E-W	18	...	...	...	0	0	0	0	0	0.06	0.06	0.06	0	0.06	0.06
IVIA6&7	N-S	12	...	...	...	0	0	0	0	0	0	0.17	0.17	0.08	0.08	0.08
	E-W	18	...	...	...	0	0	0	0	0	0	0	0	0.06	0.06	0
El Realengo	N-S	20	0.05	0.05	0.05	0.05	0	0	0	0	0	0.05	0.05	...	...	...
	E-W	20	0	0.05	0.05	0.05	0	0	0	0	0.05	0.05	0.05	...	...	...
Los Valles	N-S	17	0	0.06	0.06	0	0	0	0	0	0.06	0	0.06	0.06	0.12	0.18
	E-W	24	0	0	0	0	0	0.08	0.08	0.08	0.04	0	0	0	0	0.04

[a] Due to the irregular shape of the Orihuela plot, it was not analyzed by ordinary runs.
[b] Values shown for each plot in each year are the proportion of the number of test rows with significant aggregation ($P = 0.05$) divided by the total number of rows tested.
[c] ... = not tested.

TABLE 3. Index of dispersion (I_β) analyses for citrus tristeza virus (CTV) in five citrus orchards in eastern Spain for two quadrat sizes

Plot	Quadrat size	df	Year of assessment[a]													
			1981	1982	1983	1984	1985	1986	1987	1988	1989	1990	1991	1992	1993	1994
IVIA3&4	2 × 2	53	...[b]	...	...	0.976	0.946	0.932	0.916	0.886	1.120	1.082	1.301	1.345	1.525	1.428
						0.524	0.585	0.616	0.647	0.707	0.256	0.317	0.069	0.048	0.008	0.022
	4 × 4	14	...	...	...	0.761	1.016	1.222	1.049	1.006	0.831	0.648	1.083	1.009	1.383	1.165
						0.714	0.433	0.251	0.400	0.443	0.639	0.827	0.367	0.441	0.142	0.295
IVIA6&7	2 × 2	53	...	...	...	0.976	0.946	0.946	1.281	1.122	0.982	1.348	1.428	1.525	1.681	1.085
						0.524	0.585	0.585	0.082	0.252	0.512	0.046	0.022	0.008	0.001	0.312
	4 × 4	14	...	...	...	1.438	1.016	1.016	1.579	1.341	1.279	2.131	2.131	2.349	3.364	2.089
						0.126	0.433	0.433	0.077	0.173	0.211	0.008	0.008	0.003	0.000	0.010
El Realengo	2 × 2	99	1.086	1.022	1.074	1.149	1.048	0.979	0.997	0.990	0.956	1.061	1.082	...	...	
			0.262	0.420	0.289	0.148	0.352	0.542	0.491	0.510	0.597	0.321	0.271			
	4 × 4	24	1.360	1.019	1.074	0.943	1.119	0.948	0.972	0.959	0.958	0.964	1.180	...	...	
			0.112	0.436	0.364	0.542	0.312	0.535	0.501	0.512	0.524	0.512	0.246			
Los Valles	2 × 2	107	0.932	0.855	0.903	0.903	0.903	1.169	1.169	1.169	1.235	1.127	1.110	1.110	1.138	1.209
			0.678	0.717	0.754	0.754	0.754	0.111	0.111	0.111	0.050	0.175	0.205	0.205	0.156	0.070
	4 × 4	29	0.782	0.716	0.905	0.682	0.682	1.167	1.684	1.684	2.174	1.570	1.389	1.389	1.155	1.353
			0.792	0.870	0.613	0.902	0.902	0.246	0.012	0.012	0.000	0.026	0.080	0.080	0.258	0.097
Orihuela	2 × 2	88	...	...	...	...	0.858	0.882	0.882	0.890	1.1017	0.961	0.935	0.976	0.953	1.559
							0.827	0.778	0.778	0.761	0.436	0.585	0.653	0.543	0.605	0.000
	4 × 4	21	...	...	...	...	1.179	0.907	0.907	1.459	1.588	1.618	1.444	1.722	1.571	2.240
							0.258	0.583	0.583	0.080	0.043	0.037	0.086	0.021	0.046	0.001

[a] Index of dispersion (I_β) and associated probability (P) values for the indicated quadrat sizes by year for citrus plots in eastern Spain infected with CTV. Values presented for each assessment date are I_β (=observed variance/binomial variance) and P (=significance probability). P values were calculated by comparison of df × I_β with the chi-squared distribution. Values of I_β not significantly different from 1 ($0.95 > P > 0.05$) indicate that the pattern of diseased trees is indistinguishable from random. A large (>1) I_β and a small P (≤0.05) suggest rejection of H_0 (random pattern) in favor of H_1 (aggregated pattern of diseased trees).
[b] No assessment data were available for the year or too few data points were available to allow calculation. For all plots and assessment years, incidence of diseased trees was determined by a polyclonal enzyme-linked immunosorbent assay test for CTV.

were partitioned into 2 × 2-, 4 × 4-, and, where possible, 8 × 8-tree quadrats, depending on the spatial dimensions of each plot. The index of dispersion (I_β) associated with the beta-binomial distribution was used to test for the presence of aggregation at each tree-quadrat size (32,35). For the beta-binomial index, a large I_β (>1) combined with a small P (≤0.05) suggests aggregation of diseased trees (32).

Analytical techniques based on infected-tree position were employed to examine the data for more complex spatial patterns and spatial associations over longer distances. Because the serological confirmations of disease resulted in simple binary data for each tree, (i.e., + or – CTV), 2DCLASS and STCLASS analyses were used to examine the spatial patterns of diseased and healthy plants with the STCLASS computer program for personal computers (43). The observed standardized count frequency (SCF) for each $[X,Y]$ distance class was compared to expected SCFs, estimated by 400 computer simulations using a Monte Carlo pseudo-random function and an equal number of diseased trees randomly distributed to generate test lattices of the same dimension. Data for assessment dates were analyzed by STCLASS if they met the

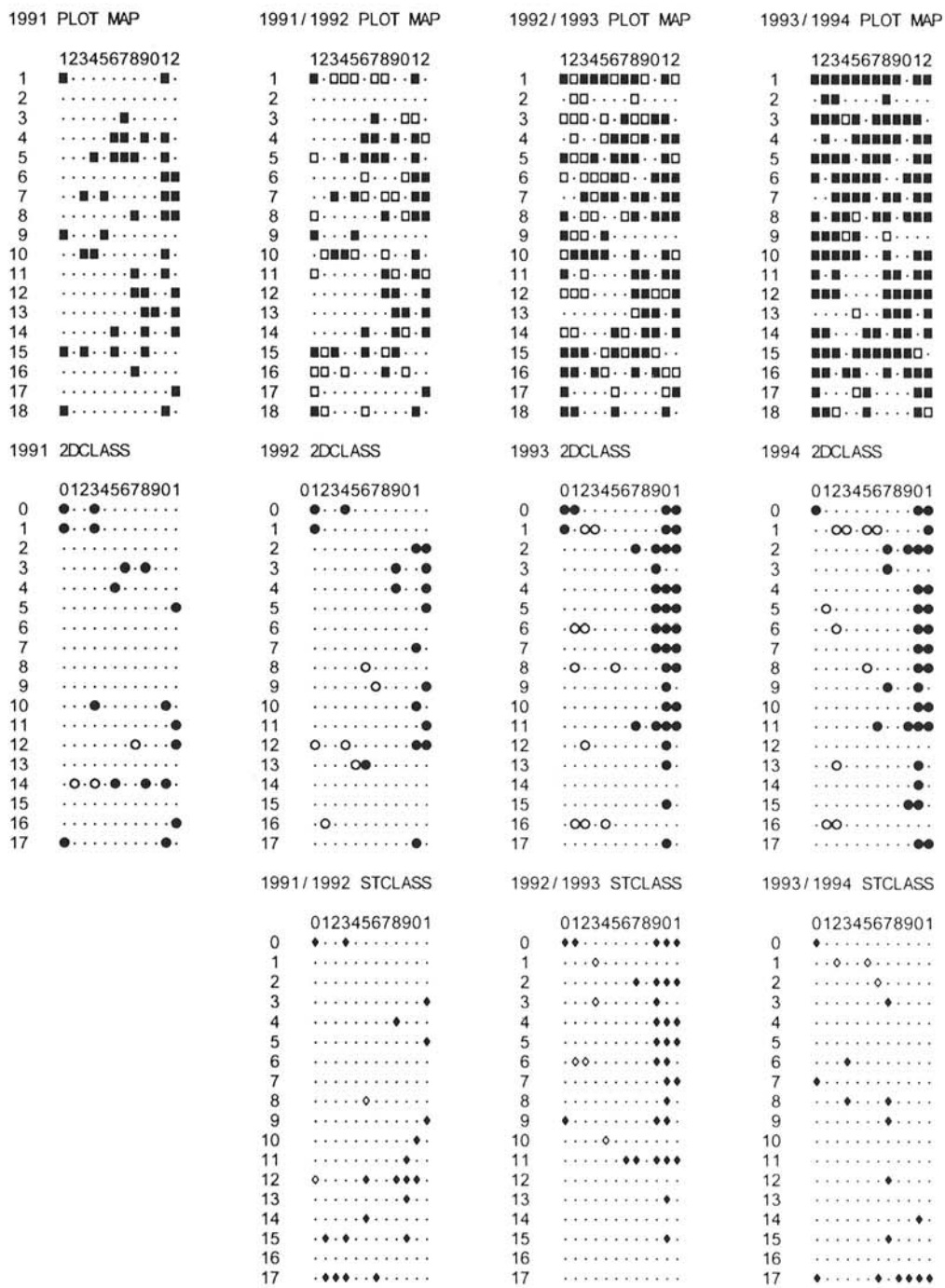

Fig. 2. Spatial pattern maps of citrus tristeza virus (CTV) (first row) with associated two-dimensional distance (2DCLASS) proximity patterns (second row) and associated spatio-temporal distance class (STCLASS) proximity patterns (third row) for plot IVIA3&4 in eastern Spain by year. Spatial patterns were determined by enzyme-linked immunosorbent assay using monoclonal antibodies for CTV. First row: Black and white squares and smaller black dots indicate position of CTV-positive trees for the first year of the comparison, CTV-positive trees for the second year of the comparison, and CTV-negative trees, respectively. Second row: Proximity pattern matrices from 2DCLASS analyses. Black and white circles and small black dots indicate $[X,Y]$ distance classes with standardized count frequencies (SCF) greater than expected, less than expected, and as expected, respectively ($P < 0.05$). Third row: Proximity pattern matrices from STCLASS analyses. Black and white diamonds and small black dots indicate $[X,Y]$ distance classes with SCF greater than expected, less than expected, and as expected, respectively ($P < 0.05$).

requirements for this analysis: $0.15 \leq y \leq 0.80$, where y = disease incidence. 2DCLASS and STCLASS proximity patterns were interpreted as random if the number of significant SCFs was <25% and aggregated if the number of significant SCFs was ≥25%. Core clusters were interpreted as groupings of significantly greater than expected $[X,Y]$ distance classes that formed a discrete and contiguous group with the origin, i.e., distance class [0,0] (43,45). The data set was interpreted as having significant edge effects if >12.5% of the $[X,Y]$ distance classes in the distal (outermost) row and column of the proximity pattern had significantly greater than expected SCF values (43,44,45). STCLASS proximity patterns also were generated by the STCLASS program. These were used to compare the spatial relationships among CTV-positive trees between two assessment dates for which there was a change in disease incidence of ≥0.05. Graphic representations of the proximity patterns were prepared from the 2DCLASS and STCLASS analyses and output to visualize the results.

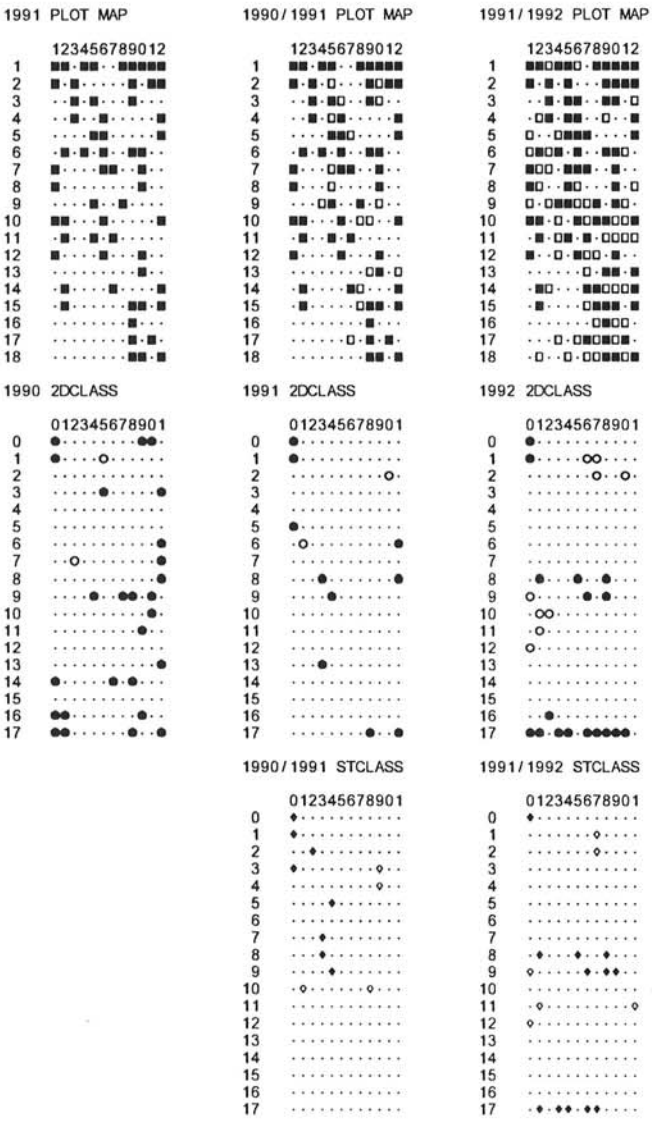

Fig. 3. Spatial pattern maps of citrus tristeza virus (CTV) (first row) with associated two-dimensional distance (2DCLASS) proximity patterns (second row) and associated spatio-temporal distance class (STCLASS) proximity patterns (third row) for plot IVIA6&7 in eastern Spain by year. Spatial patterns were determined by enzyme-linked immunosorbent assay using monoclonal antibodies for CTV. First row: Black and white squares and smaller black dots indicate position of CTV-positive trees for the first year of the comparison, CTV-positive trees for the second year of the comparison, and CTV-negative trees, respectively. Second row: Proximity pattern matrices from 2DCLASS analyses. Black and white circles and small black dots indicate $[X,Y]$ distance classes with standardized count frequencies (SCF) greater than expected, less than expected, and as expected, respectively ($P < 0.05$). Third row: Proximity pattern matrices from STCLASS analyses. Black and white diamonds and small black dots indicate $[X,Y]$ distance classes with SCF greater than expected, less than expected, and as expected, respectively ($P < 0.05$).

Geostatistical analysis was used to further examine the spatio-temporal relationships among CTV-positive trees over the duration of the individual epidemics and to augment STCLASS analysis. Data sets for each plot were prepared for analysis by assigning diseased trees a temporal value (n) based on the number of years infected relative to the final assessment year. For example, if two trees were CTV-positive for the final 7 and 10 years of the epidemic, they were assigned temporal values of $n = 7$ and 10, respectively. If a tree remained uninfected for the duration of the time during which the epidemic was monitored, then $n = 0$. Thus, an individual tree was quantitatively weighted more heavily if it became infected earlier in the epidemic. Geostatistical analysis was performed using GS+/386 geostatistical software (version 2.16, Gamma Design Software, Plainwell, MI) for 0° (omnidirectional with an angle of inclusion of 180°) and 0, 45, 90, and 135° relative to the rows in each plot with an angle of inclusion of 90°. The semivariance $\gamma(h)$ (the variance about the mean difference in disease between all sampling units for a given distance) versus distance in meters was plotted (13,33,47). Linear, linear with sill, exponential, spherical, and Gaussian transitional models, commonly used in geostatistical analysis, were fit to the semivariance $\gamma(h)$ versus distance data by means of nonlinear regression analysis performed via a GS+ model-fitting subroutine (15, 16,38). The resulting two-dimensional spatio-temporal structure is considered anisotropic when directional semivariograms diverge from one another over distance (49).

RESULTS

Analysis of temporal disease progress. CTV was first detected in the two IVIA and one Orihuela plots in 1984 6 and 5 years after planting, respectively. In the remaining plots, CTV was already present when the surveys began. Epidemics of CTV progressed over several years. For the plots studied, disease progress was in a linear or logarithmic phase of increase for the preponderance of the assessment years, and an asymptote of disease was approached only for the IVIA6&7 plot (Fig. 1). Therefore, asymptotic models were not appropriate for four of the five plots studied, and simpler models were sought to better describe CTV progress over time. The simplest model capable of adequately describing the temporal data was sought. A linear model described well the data for the El Realengo and Orihuela plots, whereas an exponential model described well disease progress for the IVIA3&4, IVIA6&7, and Los Valles plots. For the IVIA6&7 plot, an asymptote of disease was approached and thus, a logistic or Gompertz model was appropriate (Table 1).

Analysis of spatial arrangement of diseased trees. Aggregation within- and across-rows was rarely detected in any of the CTV plots for various assessment years by ordinary runs analysis, indicating that CTV-positive trees did not influence the condition of adjacent trees (Table 2). Due to the odd shape of the plot and the numerous missing trees, ordinary runs analysis was not performed for the Orihuela plot. There was no consistent or significant association with direction of spread in any of the plots examined, which indicated that CTV-positive trees were not necessarily associated with trees immediately adjacent. Interpretation of the I_β index of dispersion values suggested nonsignificant aggregation, i.e., random spatial structure, of CTV-positive trees for most plots and quadrat sizes over time (Table 3). However, statistically significant and large I_β values, when they occurred, were associated with years during the middle of and late in the assessment period. With the exception of the IVIA6&7 plot, when aggregation was indicated over a period of assessments, disease incidence remained low and changed very little over time. Values for I_β for the IVIA6&7

plot suggested aggregation of CTV-positive trees in 2 × 2 and 4 × 4 quadrats for 1990 to 1993, during which time disease incidence changed from 0.27 to 0.86.

The general lack of aggregation among adjacent, CTV-positive trees indicated by ordinary runs analyses combined with some indications of aggregation, as detected by I_β when trees were parceled into 2 × 2 or larger quadrats, suggested that spatial relationships over greater distances might exist in the CTV data sets and prompted the use of more detailed spatial analyses to examine spatial dependency over longer distances. 2DCLASS and STCLASS analyses resulted in distance classes with significantly greater than expected SCF values for each plot in each year (Figs. 2, 3, and 4). For 2DCLASS analyses, the number of distance classes with significantly greater than expected SCF values ranged from 3.3 to 16.7% and tended to increase over time as disease incidence increased for IVIA3&4; decrease over time for El Realengo; and decrease then increase for IVIA6&7 (Table 4). Significantly fewer than expected SCF values were less common but occurred for all plots and during all assessment periods. 2DCLASS proximity patterns were random for most plots and assessment dates and exhibited few or small core clusters, i.e. significant distance classes immediately adjacent to the origin (distance class [0,0]). Thus, aggregation of immediately adjacent trees was infrequent and not extensive where it occurred (Figs. 2, 3, and 4; Table 4) compared to the number of SCFs encountered at further distance classes. Reflected clusters, groups of significant SCFs discontinuous with the core clusters, occurred for all plots and assessment dates. Reflected clusters varied from 2 to 30 SCFs in size; however, small reflected clusters of 2 to 3 SCFs were most common (Figs. 2, 3, and 4). Significant edge effects in the 2DCLASS proximity patterns were indicated for IVIA3&4 and IVIA6&7 but not for the El Realengo plot. Although all 2DCLASS proximity patterns were considered nonrandom, the strength of nonrandomness was low. The associated proximity indices indicated that the few core clusters that existed were tightly organized (Table 4).

For the STCLASS analyses, the change in mapped disease incidence between two assessment dates was examined. For those situations in which STCLASS analysis was appropriate, the number of distance classes with significantly greater than expected SCF values ranged from 4.2 to 23.3% and were variable over time (Table 5). As with the 2DCLASS analyses, significantly less than expected SCF values were less common. The majority of the spatio-temporal proximity patterns were random, and corresponding values for the strength of nonrandomness were low (Table 5). Core clusters existed for less than half of the possible assessment date comparisons, whereas numerous reflected clusters were found in all spatio-temporal proximity patterns and ranged in size, with reflected clusters of two to four SCFs being the most common (Figs. 2, 3, and 4; Table 5). Because core clusters never exceeded two SCFs, the proximity index was maximal (1.0) where core clusters existed or minimal (0) where they did not exist (Table 5). Edge effects were significant for all but one proximity pattern comparison, i.e., IVIA6&7 for 1990 compared to 1991 (Table 5;

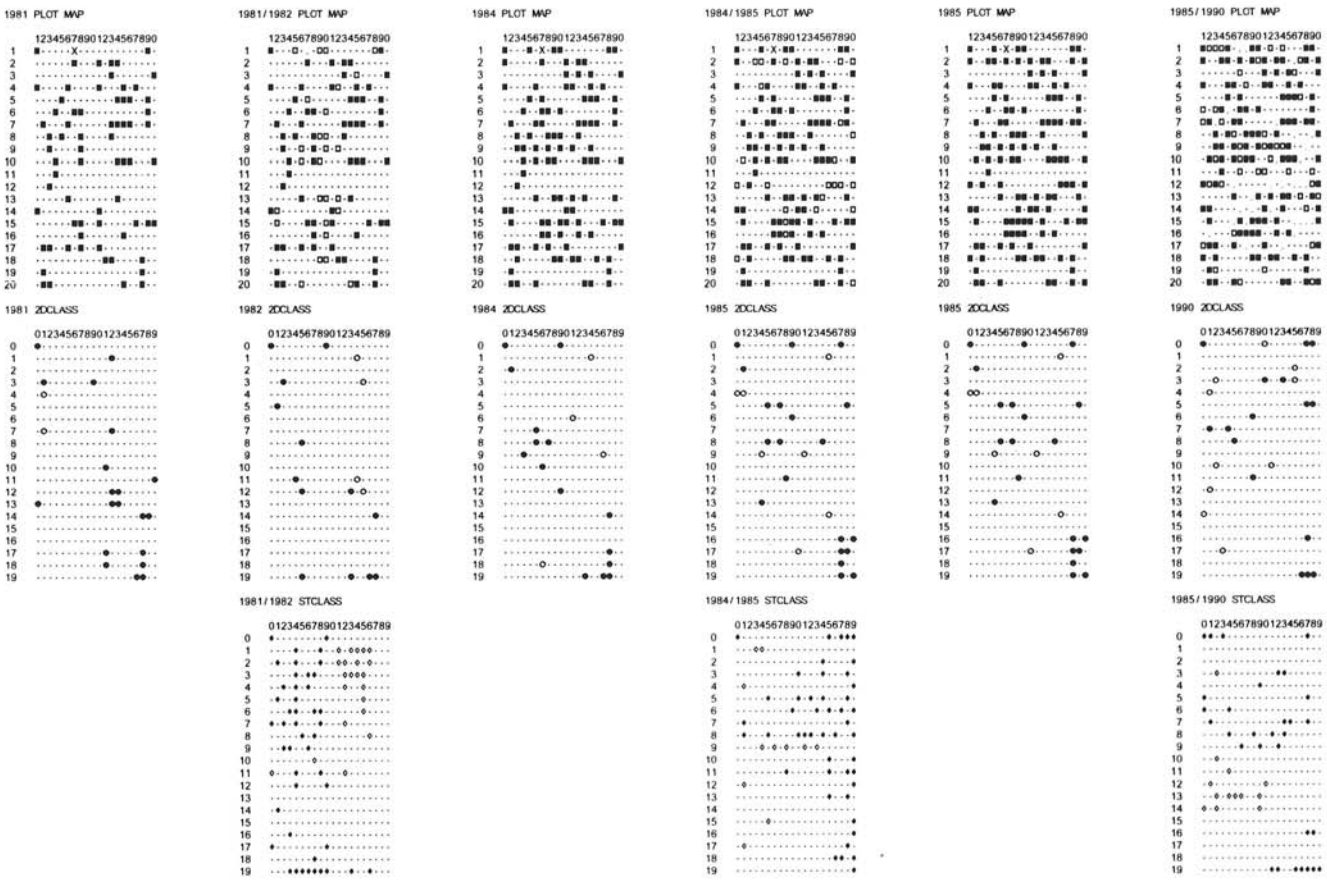

Fig. 4. Spatial pattern maps of citrus tristeza virus (CTV) (first row) with associated two-dimensional distance (2DCLASS) proximity patterns (second row) and associated spatio-temporal distance class (STCLASS) proximity patterns (third row) for El Realengo plot in eastern Spain by year. Spatial patterns were determined by enzyme-linked immunosorbent assay using monoclonal antibodies for CTV. First row: Black and white squares and smaller black dots indicate position of CTV-positive trees for the first year of the comparison, CTV-positive trees for the second year of the comparison, and CTV-negative trees, respectively. Second row: Proximity pattern matrices from 2DCLASS. Black and white circles and small black dots indicate $[X,Y]$ distance classes with standardized count frequencies (SCF) greater than expected, less than expected, and as expected, respectively ($P < 0.05$). Third row: Proximity pattern matrices from STCLASS analyses. Black and white diamonds and small black dots indicate $[X,Y]$ distance classes with SCF greater than expected, less than expected, and as expected, respectively ($P < 0.05$).

Figs. 2, 3, and 4).

Semivariograms of the CTV spatio-temporal data sets, when fitted to several traditional transitional models via the GS+ model-fitting routines (15), resulted in a low coefficient of determination of nonlinear regression for most models tested (data not shown). As a result, no generalized model was deemed appropriate or representative of CTV spatio-temporal semivariance over distance. Most of the graphs showed a linear relationship between semivariance and distance that was interpreted as a general lack of aggregation, i.e., randomness, of CTV-positive trees over time. No appreciable anisotropy existed for IVIA3&4, IVIA6&7, and El Realengo spatio-temporal data sets. A small amount of anisotropy did exist for Los Valles and Orihuela data sets but only at the greatest lag distances for which fewer pairs of diseased trees existed for comparison (Fig. 5).

DISCUSSION

The main goals of the spatio-temporal studies were to determine the relationship of diseased trees to each other, whether there was any directionality to disease spread, and the size and shape of patterns of diseased trees. Each of these characteristics provides evidence of the underlying process of disease spread, i.e., vector movement or horticultural practices that might influence disease spread.

Temporal progress of tristeza in orange orchards was adequately represented by a linear model when disease incidence remained low, <0.10, whereas exponential models were useful when disease incidence continued to increase. In the one case in which an asymptote of disease was approached, a logistic or Gompertz model was most appropriate. For the single grapefruit or-

TABLE 4. Statistics from two-dimensional distance class analysis for citrus tristeza virus (CTV) in citrus orchards in eastern Spain

Plot	Date	Disease incidence[a]	No. significant[b]		Proximity pattern[c]	Strength of nonrandomness[d]	Core cluster size[e]	No. of reflected clusters[f]	Reflected cluster size[g]	Proximity index[h]	Edge effect[i]
			SCF+	SCF–							
El Realengo	1981	0.173	20	3	R	0.06	0	4	2–6	0	n.s.
(n = 400)	1982	0.240	19	5	R	0.06	0	4	2–3	0	n.s.
	1984	0.273	15	6	R	0.05	0	2	2–4	0	n.s.
	1985	0.328	13	9	R	0.06	0	1	4	0	n.s.
	1990	0.403	16	10	R	0.07	0	4	2–3	0	n.s.
IVIA3&4	1991	0.208	17	3	R	0.09	2	4	2–3	1	+
(n = 216)	1992	0.356	17	6	R	0.11	2	2	5	1	+
	1993	0.588	36	10	R	0.21	3	1	30	0.75	+
	1994	0.630	32	10	R	0.19	0	4	2–16	0	+
IVIA6&7	1990	0.278	25	2	R	0.13	2	5	2–6	1	+
(n = 216)	1991	0.356	9	2	R	0.05	2	1	2	1	+
	1992	0.588	16	9	R	0.12	2	4	2–5	1	+

[a] Number of CTV-positive trees/n, where n = total number of trees in the orchard.
[b] Number of [X,Y] distance classes with standardized count frequencies (SCFs) significantly greater (SCF+) or less (SCF–) than expected.
[c] R = indistinguishable from random (number of significant SCFs < 25%), N = nonrandom, i.e., aggregated (number of significant SCFs ≥ 25%).
[d] A function of the proportion of the SCFs [(SCF+) + (SCF–)] in the matrix.
[e] The number of significant SCF+ distance classes contiguous with the origin that form a discrete group.
[f] The number of clusters of SCF+ distance classes within the proximity pattern that are noncontiguous with the origin or core clusters.
[g] The range of cluster sizes, i.e., number of SCF+ in each cluster.
[h] An estimate of the 'density' of the core cluster, calculated as the proportion of SCF+ within the area circumscribed by the outer row and column limits of the core cluster.
[i] + indicates the proportion (number of significant SCF+ distance classes/total number of edge distance classes) occurring at the two edges of the proximity pattern farthest from the origin (i.e., the outermost row and column of the distance class matrix) is ≥0.125; n.s. = nonsignificant.

TABLE 5. Statistics from spatio-temporal distance class analysis for citrus tristeza virus in citrus orchards in eastern Spain

Plot[a]	Assessments years compared[b]	Disease incidence[c]	No. of infections[d]	No. significant[e]		Proximity pattern[f]	Strength of nonrandomness[g]	Core cluster size[h]	No. of reflected clusters[i]	Reflected cluster size[j]	Proximity index[k]	Edge effect[l]
				SCF+	SCF–							
El Realengo	1981–1982	0.17–0.24	27	37	23	R	0.15	0	9	2–11	0	+
(n = 400)	1984–1985	0.27–0.32	24	49	11	R	0.15	0	11	2–8	0	+
	1985–1990	0.33–0.40	42	30	13	R	0.11	2	7	2–5	1	+
IVIA3&4	1991–1992	0.21–0.36	32	20	2	R	0.10	0	2	3–7	0	+
(n = 216)	1992–1993	0.36–0.59	50	30	5	N	0.16	2	4	2–17	1	+
	1993–1994	0.59–0.63	9	15	3	R	0.08	0	2	2–4	0	+
IVIA6&7	1990–1991	0.29–0.36	17	7	4	R	0.05	2	1	2	1	n.s.
(n = 216)	1991–1992	0.36–0.59	50	11	6	N	0.08	0	4	2–3	0	+

[a] For each plot n = the number of trees in the matrix.
[b] Spatio-temporal comparisons were made between the years indicated.
[c] Disease incidence for each of the years indicated.
[d] The number of new infections that occurred between the years indicated.
[e] Number of [X,Y] distance classes with standardized count frequencies (SCFs) significantly greater (SCF+) or less (SCF–) than expected.
[f] R = not distinguishable from random (number of significant SCFs < 25%); N = nonrandom, i.e., aggregated (number of significant SCFs ≥ 25%).
[g] Function of the proportion of the SCFs [(SCF+) + (SCF–)] in the matrix.
[h] The number of significant SCF+ distance classes contiguous with the origin that form a discrete group.
[i] The number of clusters of SCF+ distance classes within the proximity pattern that are noncontiguous with the origin or core clusters.
[j] The range of cluster sizes, i.e., number of SCF+ in each cluster.
[k] An estimate of the 'density' of the core cluster calculated as the proportion of SCF+ within the area circumscribed by the outer row and column limits of the core cluster.
[l] + indicates that the proportion (number of significant SCF+ distance classes/total number of edge distance classes) occurring at the two edges of the proximity pattern farthest from the origin (i.e., the outermost row and column of the distance class matrix) was ≥ 0.125; n.s. = nonsignificant.

chard, disease increase was linear even when disease incidence was >0.1. For grapefruit, a logarithmic increase was not seen. This linear aspect of CTV disease increase for grapefruit in Spain is consistent with CTV increase measured in grapefruit orchards in Florida (T. R. Gottwald, *unpublished data*). Although linear and exponential models are adequate for describing the temporal increase of CTV, they are only approximations of real-world events and tend to smooth out fluctuations in CTV increases associated with virus transmission from year to year. Aphid populations, which are subject to a variety of environmental influences, are not uniform from one year to the next (30,31,48,57). The fluctuations in vector populations and the differences in transmission rate of CTV that might result could be responsible for the temporal changes in CTV, which often deviates from the predicted smooth curves of disease increase over time.

In general, randomness of CTV incidence among immediately adjacent trees was indicated for the majority of plots and assessment periods by ordinary runs. However, this general lack of similarity of disease status among immediately adjacent trees (i.e., randomness) for assessment dates early in the epidemics, determined by ordinary runs, is not indicative of a lack of spatial processes that might occur over longer distances. Beta-binomial spatial analyses indicated a prevalence of nonrandom spatial structures for data partitioned into 2 × 2 and 4 × 4 quadrats.

2DCLASS and spatio-temporal analyses generally confirmed the lack of aggregation among immediately adjacent trees and suggested that the spatial patterns were generally random. Because the serological confirmations resulted in binary data (i.e., +/–) for CTV incidence, the distance classes are directly related to the distances between trees. Core clusters of SCFs were few and limited in size for nearly all plots and assessment dates, which confirms the general lack of aggregation. The indication of significant edge effects for 2DCLASS and STCLASS analyses for many of the plots suggests that inoculum from areas outside the plots may have influenced the spatial patterns and their change over time.

Spatial and spatio-temporal structures of disease, which are generally devoid of aggregation but which are random or have spatial associations over longer distances, are often complex and difficult to interpret compared to aggregated structures. Such structures are not prevalent in phytopathological literature. STCLASS analyses indicated a general lack of aggregation, and we were hesitant to draw conclusions based on STCLASS results alone without further corroboration. Thus, the spatio-temporal geostatistical analysis was important because it allowed examination of the spatial

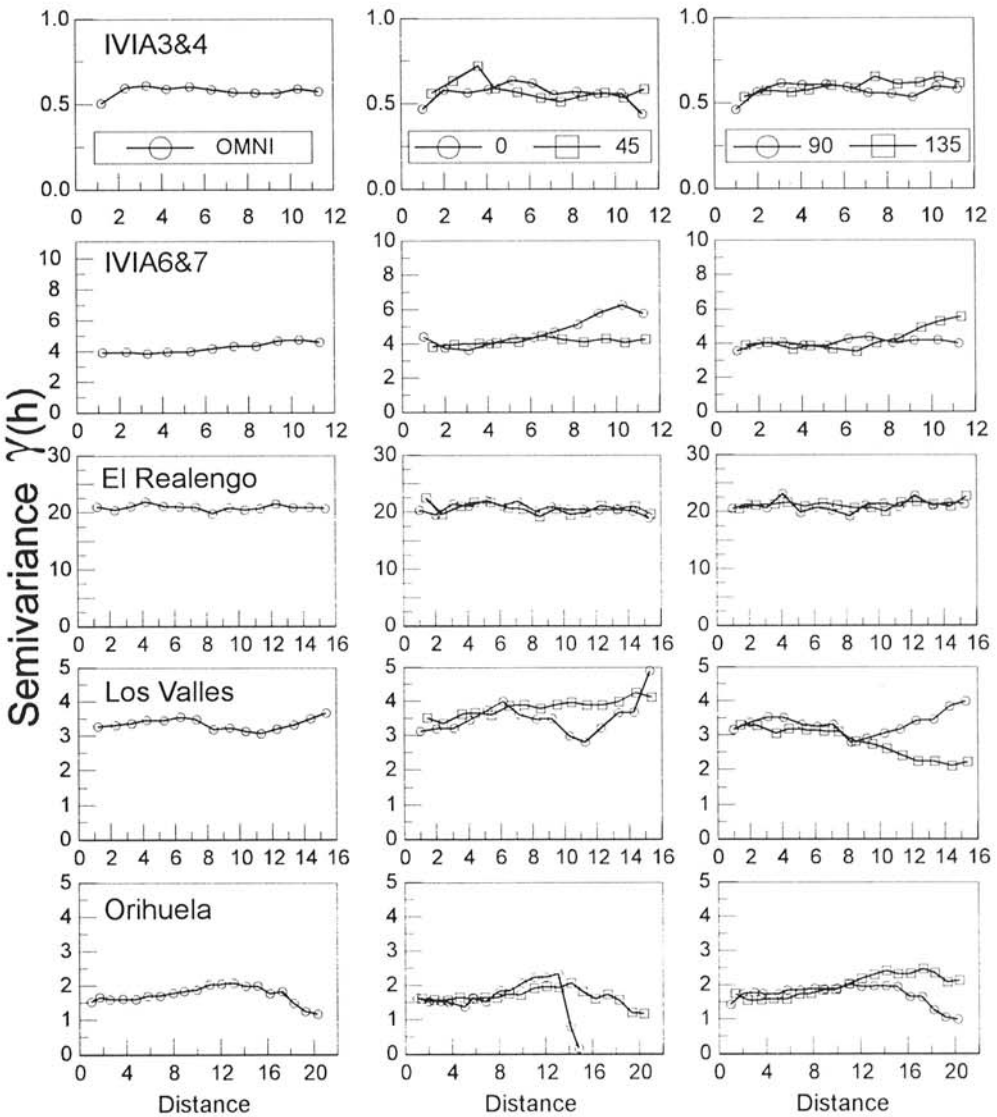

Fig. 5. Spatio-temporal geostatistics analysis results for citrus tristeza virus (CTV) increase in five citrus orchards in eastern Spain. Nonoriented and oriented semivariograms (orientation indicated) from geostatistical analyses for CTV disease spread measured at 1-tree intervals. For this analysis, CTV-positive trees were weighted based on the number of years infected relative to the final year of assessment.

structure of each plot over all assessment dates in a single analysis, whereas STCLASS analysis provided comparison only between two assessment dates. The transitional models often used in geostatistics assume lower order spatial associations that degrade over distance as expected in situations of aggregated disease. The poor fit of these transitional models due to the linear nature of the semivariance measured confirmed the general lack of aggregation among CTV-positive trees and suggested a random spatio-temporal structure. Therefore, geostatistical analysis of CTV spatio-temporal data sets confirmed the lack of spatial dependency of CTV-positive trees over time.

In the majority of cases, there was no clear evidence that anisotropy of CTV-positive trees existed through time within the Spanish orchards. Geostatistical analyses of the Spanish CTV epidemics did not demonstrate longer distance associations among CTV-positive trees. If longer distance associations had existed where aggregation did not, then semivariance graphs should have depressions or 'valleys' in otherwise linear semivariance plots, which they did not. Therefore, longer distance associations, which were one possible interpretation of beta-binomial distribution results, were not confirmed by spatio-temporal geostatistical analyses.

The orchards studied were CTV-free when established, and thus, CTV was introduced and spread within the plots probably by multiple events over the years. Therefore, we assume that the spatial relationships of infected trees to one another are indicative of the most likely distances over which transmission of the virus is most prevalent. We suggest two possible and perhaps interacting factors that could lead to the spatial and spatio-temporal patterns of CTV observed. First, the random spatial patterns indicated by ordinary runs and beta-binomial analyses and lack of spatio-temporal dependency among adjacent trees indicated by 2DCLASS and STCLASS could be due to exogenous sources of CTV. The significant edge effects detected in both 2DCLASS and STCLASS proximity patterns further suggest that this might be the case. Second, CTV may have been transmitted within the confines of the plots as well, even though transmission to adjacent trees was rare. We feel that both inter- and intraplot transmission of CTV may have taken place, most likely resulting from multiple transmission events or episodes over the multiyear duration of the epidemics studied.

These findings provide insight into the underlying processes of CTV spread. From our findings, we could not reject the null hypothesis that CTV spatial arrangement is random, at least for the spatial scales studied. Spread does not appear to occur in immediately adjacent trees. Therefore, CTV must spread to locations several trees away or over even larger spatial scales. This would explain the general lack of aggregation found in ordinary runs analysis and in the beta-binomial index of dispersion analyses and the lack of adjacent-tree spatio-temporal dependency seen in STCLASS and geostatistical analyses. This also may be related to vector biology and feeding habits. The migratory habits of *A. gossypii* in citrus could account for a portion, if not all, of the spatial spread of CTV observed in the plots studied in Spain, much as it has been shown to do in California (17,18,57) and is assumed to do in other areas where it and citrus coexist (2,46, 48,55). Therefore, if a nonrandom spatial structure of CTV incidence does exist, it may well be of a complexity beyond the ability of the spatial analysis methods employed of a larger or perhaps regional scale and beyond the dimensions of the plots studied.

LITERATURE CITED

1. Ballester-Olmos, J. F., Pina, J. A., Carbonell, E. A., Moreno, P., Hermoso de Mendosa, A., Cambra, M., and Navarro, L. 1993. Biological diversity of citrus tristeza (CTV) isolates in Spain. Plant Pathol. 42:219-229.
2. Bar-Joseph, M., and Loebenstein, G. 1972. Effects of strain, source plant, and temperature on transmissibility of citrus tristeza virus by the melon aphid. Phytopathology 63:716-720.
3. Bar-Joseph, M., Roccah, B., and Loebenstein, G. 1977. Evaluation of the main variables that affect citrus tristeza virus transmission by aphids. Proc. Int. Soc. Citricult. 3:958-961.
4. Berger, R. D. 1981. Comparison of the Gompertz and logistic equations to describe plant disease progress. Phytopathology 71:716-719.
5. Cambra, M. 1994. El virus de la tristeza de los cítricos. Nueva situaeíon en la Comunidad Valenciana. Phytoma España 58:26-31.
6. Cambra, M., Camarasa, E., Gorris, M. T., Garnsey, S. M., and Carbonell, E. 1991. Comparison of different immunosorbent assays for citrus tristeza virus (CTV) using CTV-specific monoclonal and polyclonal antibodies. Pages 38-45 in: Proc. 11th Conf. Int. Org. Citrus Virol. R. H. Brlansky, R. F. Lee, and L. W. Timmer, eds. International Organization of Citrus Virologists, Riverside, CA.
7. Cambra, M., Camarasa, E., Gorris, M. T., Garnsey, S. M., Gumpf, D. J., and Tasi, M. C. 1993. Epitope diversity of citrus tristeza virus isolates in Spain. Pages 33-38 in: Proc. 12th Conf. Int. Org. Citrus Virol. P. Moreno, J. V. De Graça, and L. W. Timmer, eds. International Organization of Citrus Virologists, Riverside, CA.
8. Cambra, M., Garnsey, S. M., Permar, M. A., Henderson, C. T., Gumpf, D. J., and Vela, C. 1990. Detection of citrus tristeza virus (CTV) with a mixture of monoclonal antibodies. (Abstr.) Phytopathology 80:1034.
9. Cambra, M., Serra, J., Bonet, J. C., and Villalba, D. 1990. Situación de la tristeza de los cítricos en la Comunidad Valenciana. Serie Fullets Divulgació 30. Ed. Generalitat Valenciana. Conselleria d'Agricultura I Pesca, Valencia, Spain.
10. Cambra, M., Serra, J., Villalba, D., and Moreno, P. 1988. Present situation of the citrus tristeza virus in the Valencian Community. Pages 1-7 in: Proc. 10th Conf. Int. Org. Citrus Virol. L. W. Timmer, S. M. Garnsey, and L. Navarro, eds. International Organization of Citrus Virologists, Riverside, CA.
11. Campbell, C. L., and Madden, L. V. 1990. Introduction to plant disease epidemiology. John Wiley & Sons, New York.
12. Campbell, C. L., and Noe, J. P. 1985. The spatial analysis of soilborne pathogens and root diseases. Annu. Rev. Phytopathol. 23:129-148.
13. Chellemi, D. O., Rohrbach, K. G., Yost, R. S., and Sonoda, R. M. 1988. Analysis of the spatial pattern of plant pathogens and diseased plants using geostatistics. Phytopathology 78:221-226.
14. Chellemi, D. O., Sonoda, R. M., Pelosi, R. R., and Cohen, M. 1991. Temporal and spatial comparisons between epidemics of citrus blight and citrus tristeza virus. Pages 289-296 in: Proc. 11th Conf. Int. Org. Citrus Virol. R. H. Brlansky, R. F. Lee, and L. W. Timmer, eds. International Organization of Citrus Virologists, Riverside, CA.
15. Cressie, N. 1985. Fitting variogram models by weighted least squares. Math. Geol. 17:563-586.
16. Cressie, N. 1988. Spatial prediction and ordinary kriging. Math. Geol. 20:405-421.
17. Dickson, R. C., Flock, R. A., and Johnson, M. McD. 1951. Insect transmission of citrus quick decline virus. J. Econ. Entomol. 44:172-176.
18. Dickson, R. C., Johnson, M. McD., Flock, R. A., and Laird, E. F., Jr. 1956. Flying aphid populations in Southern California citrus groves and their relation to the transmission of the tristeza virus. Phytopathology 46: 204-210.
19. Fishman, S., Marcus, R., Talpaz, H., Bar-Joseph, M., Oren, Y., Salomon, R., and Zohar, M. 1983. Epidemiological and economic models for spread and control of citrus tristeza virus disease. Phytoparasitica 11:39-49.
20. Forner, J. B., and Piña, J. A. 1992. Plantones tolerantes a tristeza. Veinte años de historia. (I) Patrones. Levante Agríc. 31:88-92.
21. Garnsey, S. M., and Cambra, M. 1991. Enzyme-linked immunosorbent assay (ELISA) for citrus pathogens. Pages 193-216 in: Graft Transmissible Diseases of Citrus. C. N. Roistacher, ed. United Nations, Food and Agricultural Organization, Rome.
22. Gottwald, T. R., Aubert, B., and Zhao, X.-Y. 1989. Preliminary analysis of citrus greening (Huanglungbin) epidemics in the People's Republic of China and French Reunion Island. Phytopathology 79:687-693.
23. Gottwald, T. R., Llácer, G., Aviñent, L., Hermoso de Mendosa, A., and Cambra, M. 1995. Analysis of the spatial spread of Sharka (Plum pox virus) in apricot and peach orchards in eastern Spain. Plant Dis. 79:266-278.
24. Gottwald, T. R., Cambra, M., and Moreno, P. 1993. The use of serological assays to monitor spatial and temporal spread of citrus tristeza virus in symptomless trees in eastern Spain. Pages 51-61 in: Proc. 12th Conf. Int. Org. Citrus Virol. P. Moreno, J. V. De Graça, and L. W. Timmer, eds. International Organization of Citrus Virologists, Riverside, CA.
25. Gottwald, T. R., and Graham, J. H. 1990. Spatial pattern analysis of epidemics of citrus bacterial spot in Florida citrus nurseries. Phytopathology 80:181-190.
26. Gottwald, T. R., McGuire, R. G., and Garran, S. 1988. Asiatic citrus canker: Spatial and temporal spread in simulated new planting situations in Argentina. Phytopathology 78:739-745.

27. Gottwald, T. R., Timmer, L. W., and McGuire, R. G. 1991. Analysis of disease progress of citrus canker in nurseries in Argentina. Phytopathology 79:1276-1283.
28. Hermoso de Mendoza, A., Ballester-Olmos, J. F., and Pina Lorca, J. A. 1984. Transmission of citrus tristeza virus by aphids (Homoptera, Aphidinea) in Spain. Pages 23-27 in: Proc. 9th Conf. Int. Org. Citrus Virol. S. M. Garnsey, L. W. Timmer, and J. A. Dodds, eds. International Organization of Citrus Virologists, Riverside, CA.
29. Hermoso de Mendoza, A., Ballester-Olmos, J. F., Pina, J. A., Serra, J., and Fuertes, C. 1988. Differences in transmission and efficiency of citrus tristeza virus by *Aphis gossypii* using sweet orange, mandarin or lemon trees as donor or receptor host plants. Pages 63-64 in: Proc. 10th Conf. Int. Org. Citrus Virol. L. W. Timmer, S. M. Garnsey, and L. Navarro, eds. International Organization of Citrus Virologists, Riverside, CA.
30. Hermoso de Mendoza, A., Fuertes, C., and Serra, J. 1986. Proporciones relativas y graficas de vuelo de pulgones (Homoptera:Aphidinea) en los citricos Españoles. Inv. Agrar. Prod. Prot. Veg. 1:393-408.
31. Hermoso de Mendoza, A., and Moreno, P. 1989. Cambios cuantitativos en la fauna afídica de los cítricos valencianos. Bol. San. Veg. Plagas 15: 139-142.
32. Hughes, G., and Madden, L. V. 1993. Using the beta-binomial distribution to describe aggregated patterns of disease incidence. Phytopathology 83:759-763.
33. Lecoustre, R., Fagette, D., Fauquet, C., and de Reffye, P. 1988. Analysis and mapping of the spatial spread of African Cassava mosaic virus using geostatistics and the kriging technique. Phytopathology 79:913-920.
34. Madden, L. V. 1986. Statistical analysis and comparison of disease progress curves. Pages 55-84 in: Plant Disease Epidemiology: Population Dynamics and Management. K. Leonard and W. E. Fry, eds. Macmillan Publishing, New York.
35. Madden, L. V., and Hughes, G. 1994. BBD—Computer software for fitting the beta-binomial distribution to disease incidence data. Plant Dis. 78:536-540.
36. Madden, L. V., Louie, R., Abt, J. J., and Knoke, J. K. 1982. Evaluation of tests for randomness of infected plants. Phytopathology 72:195-198.
37. Marcus, R., Fishman, S., Talpaz, H., Salomon, R., and Bar-Joseph, M. 1984. On the spatial distribution of citris tristeza virus disease. Phytoparasitica 12:45-52.
38. Matherson, G. 1963. Principles of geostatistics. Econ. Geol. 58:1246-1266.
39. Moreno, P., Navarro, L., Fuertes, C., Pina, J. A., Ballester-Olnos, J. F., Hermoso de Mendoza, A., Juárez, J., and Cambra, M. 1983. La tristeza de los agrios problemática en España. Hoja Técnica No. 47. Instituto Valenciano de Investigaciones Agrarias, Madrid.
40. Moreno, P., Piquer, J., Pina, J. A., Juárez, J., and Cambra, M. 1988. Spread of citrus tristeza virus in a heavily infested citrus area in Spain. Pages 71-76 in: Proc. 10th Conf. Int. Org. Citrus Virol. L. W. Timmer, S. M. Garnsey, and L. Navarro, eds. International Organization of Citrus Virologists, Riverside, CA.
41. Munkvold, G. P., Duthie, J. A., and Marois, J. J. 1993. Spatial patterns of grapevines with Eutypa dieback in vineyards with or without perithecia. Phytopathology 83:1440-1448.
42. Navarro, L., Juárez, J., Pina, J. A., Ballester-Olmos, J. F., and Arregui, J. M. 1988. The citrus variety improvement program in Spain (CVIPS) after eleven years. Pages 400-406 in: Proc. 10th Conf. Int. Org. Citrus Virol. L. W. Timmer, S. M. Garnsey, and L. Navarro, eds. International Organization of Citrus Virologists, Riverside, CA.
43. Nelson, S. C. 1995. Spatiotemporal distance class analysis of plant disease epidemics. Phytopathology 85:37-43.
44. Nelson, S. C., and Campbell, C. L. 1993. Comparative spatial analysis of foliar epidemics on white clover caused by viruses, fungi, and a bacterium. Phytopathology 83:288-301.
45. Nelson, S. C., Marsh, P. L., and Campbell, C. L. 1992. 2DCLASS, a two-dimensional distance class analysis software for the personal computer. Plant Dis. 76:427-432.
46. Rocha-Peña, M. A., Lee, R. F., Lastra, R., Nibblet, C. L., Ochoa-Corona, F. M., Garnsey, S. M., and Yokomi, R. K. 1995. Citrus tristeza virus and its aphid vector *Toxoptera citricida*. Plant Dis. 79:437-445.
47. Schotzko, D. J., and O'Keeffe, L. E. 1989. Geostatistical description of the spatial distribution of *Lygus hesperus* (Heteroptera:Miridae) in lentils. J. Econ. Entomol. 82:1277-1288.
48. Schwarz, R. E. 1965. Aphid-borne virus diseases of citrus and their vectors in South Africa. B. Flight Activity of citrus aphids. S. Afr. J. Agric. Sci. 8:931-940.
49. Tangmar, B. B., Yost, R. S., and Uehara, G. 1985. Application of geostatistics to spatial studies of soil properties. Adv. Agron. 38:45-94.
50. Van de Lande, H. L. 1993. Spatio-temporal analysis of spear rot and 'marchitez sorpresiva' in African palm in Surinam. Neth. J. Pathol. 99: 129-138.
51. Van der plank, J. E. 1963. Plant Diseases: Epidemics and Control. Academic Press, New York.
52. Vela, C., Cambra, M., Cortés, E., Moreno, P., Miguet, J. G., Pérez de San Román, C., and Sanz, A. 1986. Production and characterization of monoclonal antibodies specific for citrus tristeza virus and their use for diagnosis. J. Gen. Virol. 67:91-96.
53. Vela, C., Cambra, M., Sanz, A., and Moreno, P. 1986. Use of specific monoclonal antibodies for diagnosis of citrus tristeza virus. Pages 55-61 in: Proc. 10th Conf. Int. Org. Citrus Virol. L. W. Timmer, S. M. Garnsey, and L. Navarro, eds. International Organization of Citrus Virologists, Riverside, CA.
54. Vieira, S. R., Hatfield, J. L., Nielson, D. R., and Biggar, J. W. 1983. Geostatistical theory and application to variability of some agronomical properties. Hilgardia 51:1-75.
55. Yokomi, R. K., Garnsey, S. M., Civerolo, E. L., and Gumpf, D. J. 1989. Transmission of exotic citrus tristeza isolates by a Florida colony of *Aphis gossypii*. Plant Dis. 73:552-556.
56. Yokomi, R. K., Lastra, R., Stoetzel, M. B., Damsteegt, V. D., Lee, R. F., Garnsey, S. M., Gottwald, T. R., Rocha-Peña, M. A., and Nibblet, C. L. 1994. Establishment of the brown citrus aphid (Homoptera:Aphididae) in Central America and the Caribbean Basin. J. Econ. Entomol. 88:1078-1085.
57. Yokomi, R. K., and Oldfield, G. N. 1991. Seasonal fluctuations of alate aphid activity in California citrus groves. Pages 71-76 in: Proc. 11th Conf. Int. Org. Citrus Virol. R. H. Brlansky, R. F. Lee, and L. W. Timmer, eds. International Organization of Citrus Virologists, Riverside, CA.
58. Zaragoza, S. 1988. Pasado y presente de la citricultura española. Ed. Generalitat Valenciana. Conielleria d'Agricultura I Pesca, Valencia, Spain.